

# Numerical methods for random Helmholtz problem

Kai Zhang

Department of Mathematics, JLU

With Prof. G. Bao(ZJU), Prof. Y.Z. Cao(AU)  
Dr. Y.L. Hao(ZKNU) and Dr. Y. Gao(JLU)

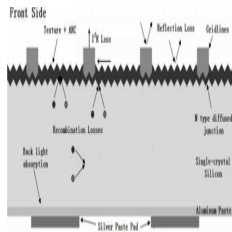
Presentation in Dynamics, Control and Numerics, FAU  
Oct 27, 2021

## Outline

- ▶ Random interface grating.
  - ▶ Expectation approximation: Taylor shape expansion.
  - ▶ Variance approximation: Low-rank Cholesky method.
- ▶ ML for inverse acoustic scattering problem.
  - ▶ Obstacle: CNN.
- ▶ Conclusions and ongoing work.

## Motivation

- (1) Grating or solar photovoltaic power generation.
- (2) Different mineral resources.



## Deterministic grating problem

Bao, Dobson and Cox 95'; Bao 95';

Chen and Wu 04'; Li, Wu and Zheng 11', etc

## Random interface

Ellipse: Canuto and Kozubek 07'; Harbrecht, Schneider and Schwab 08'; Harbrecht and Li 13'; Zhu, Hu and Wu 18'; etc.

Grating: Bao, Cao, Hao and Z 18'

Maxwell: Hao, Kang, Li and Z 18'

Acoustic scattering: Hiptmair, et al. 17'

Electromagnetic wave scattering: Hanckes and Schwab 18'

## Geometry of Helmholtz equation

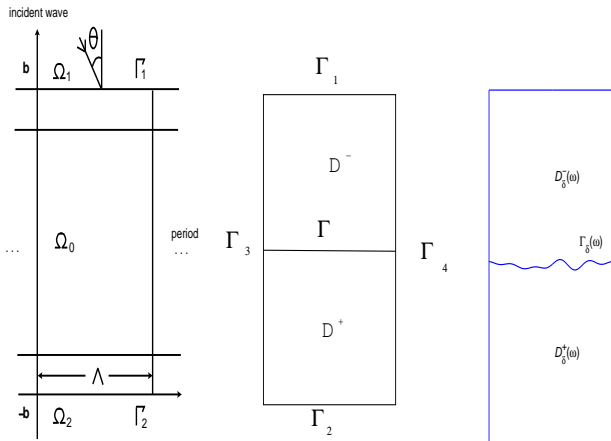


**Figure:** Deterministic grating problem, nominal interface, one realization of random interface.

Assume that an incoming plane wave

$$u_I = e^{i\alpha x_1 - i\beta_1 x_3}$$

is incident upon the grating from the top with

$$\begin{cases} \alpha = k_1 \sin \theta \\ \beta_1 = k_1 \cos \theta \end{cases}$$

and  $-\pi/2 < \theta < \pi/2$  is the angle of incidence.

We are interested in quasi-periodic solutions  $u$ , that is,

$$u_\alpha := ue^{-i\alpha x_1}$$

are  $\Lambda$  periodic. Then  $u_\alpha$  satisfies

$$\bar{\mathcal{L}}u_\alpha := (\Delta_\alpha + k^2)u_\alpha = 0,$$

where the operator  $\Delta_\alpha = \Delta + 2i\alpha\partial_{x_1} - |\alpha|^2$ .

The deterministic interface grating problem is given by:

$$\begin{aligned}\bar{\mathcal{L}}u &= \bar{g}, & \text{in } D^- \cup D^+, \\ [u] &= 0, & \text{on } \Gamma, \\ \left[ \frac{\partial u}{\partial \mathbf{n}} \right] &= 0, & \text{on } \Gamma, \\ u &= e^{-i\alpha x_1} u_I, & \text{on } \Gamma_1, \\ u &= 0, & \text{on } \Gamma_2, \\ u|_{\Gamma_3} &= u|_{\Gamma_4}, \\ \frac{\partial u}{\partial \mathbf{n}}|_{\Gamma_3} &= -\frac{\partial u}{\partial \mathbf{n}}|_{\Gamma_4}.\end{aligned}\tag{1}$$

## Nominal interface and deterministic perturbed interface.

Fix any fixed nominal interface  $\Gamma \in C^{3,1}$ , we claim  $\mathbf{n}(\mathbf{x}) \in C^{2,1}(\Gamma, \mathbb{R}^2)$ . Thus, for any

$$\kappa \in \mathcal{A} := \{ \nu \in C^{2,1}(\Gamma, \mathbb{R}^2) : \|\nu\|_{C^{2,1}(\Gamma, \mathbb{R}^2)} \leq 1 \},$$

we obtain a normal variation of the interface

$$\mathbf{V}(\mathbf{x}) := \kappa(\mathbf{x})\mathbf{n}(\mathbf{x}) \in C^{2,1}(\Gamma, \mathbb{R}^2).$$

There exists an  $\delta_0 > 0$ , such that for any  $0 \leq \delta \leq \delta_0$  the perturbed interface

$$\Gamma_\delta := \{ \mathbf{x} + \delta\kappa(\mathbf{x})\mathbf{n}(\mathbf{x}) : \mathbf{x} \in \Gamma \} \in C^{2,1}(\Gamma, \mathbb{R}^2)$$

is well defined.

## Nominal interface and random perturbed interface.

Given a random field  $\kappa \in L^2(\Omega, C^{2,1}(\Gamma, \mathbb{R}^2))$  and a perturbation amplitude  $\delta$  with  $0 \leq \delta \leq \delta_0$ , the random interface is

$$\Phi_\delta : \begin{cases} \Gamma \times \Omega \rightarrow \mathbb{R}^2, \\ (\mathbf{x}, \omega) \mapsto \mathbf{x} + \delta \kappa(\mathbf{x}, \omega) \mathbf{n}(\mathbf{x}). \end{cases}$$

A realization of the subdomains  $D_\delta^\pm(\omega)$  is thus separated by the interface

$$\Gamma_\delta(\omega) := \{\Phi_\delta(\mathbf{x}, \omega) : \mathbf{x} \in \Gamma\}, \quad \omega \in \Omega.$$

The *mean, two-point correlation function and covariance function*:

$$\mathbb{E}_{\kappa}(\mathbf{x}) := \int_{\Omega} \kappa(\mathbf{x}, \omega) dP(\omega), \quad \mathbf{x} \in \Gamma,$$

$$\text{Cor}_{\kappa}(\mathbf{x}, \mathbf{y}) := \int_{\Omega} \kappa(\mathbf{x}, \omega) \kappa(\mathbf{y}, \omega) dP(\omega), \quad \mathbf{x}, \mathbf{y} \in \Gamma,$$

$$\text{Covar}_{\kappa}(\mathbf{x}, \mathbf{y}) := \text{Cor}_{\kappa}(\mathbf{x}, \mathbf{y}) - \mathbb{E}_{\kappa}(\mathbf{x}) \mathbb{E}_{\kappa}(\mathbf{y}), \quad \mathbf{x}, \mathbf{y} \in \Gamma.$$

Assume that the random field  $\kappa(\mathbf{x}, \omega)$  is centered, namely

$$\mathbb{E}_{\kappa}(\mathbf{x}) = 0.$$

Therefore,  $\mathbb{E}(\Gamma_{\delta}(\omega)) = \Gamma$  and

$$\text{Covar}_{\kappa}(\mathbf{x}, \mathbf{y}) = \text{Cor}_{\kappa}(\mathbf{x}, \mathbf{y}).$$

The random interface grating problem:

$$\begin{aligned}
 \tilde{\mathcal{L}}u(\mathbf{x}, \omega) &= \bar{g}, & \text{in } D_\delta^-(\omega) \cup D_\delta^+(\omega), \\
 [u(\mathbf{x}, \omega)] &= 0, & \text{on } \Gamma_\delta(\omega), \\
 \left[ \frac{\partial u}{\partial \mathbf{n}}(\mathbf{x}, \omega) \right] &= 0, & \text{on } \Gamma_\delta(\omega), \\
 u(\mathbf{x}, \omega) &= e^{-i\alpha x_1} u_I, & \text{on } \Gamma_1, \\
 u(\mathbf{x}, \omega) &= 0, & \text{on } \Gamma_2, \\
 u(\mathbf{x}, \omega)|_{\Gamma_3} &= u(\mathbf{x}, \omega)|_{\Gamma_4}, \\
 \frac{\partial u}{\partial \mathbf{n}}(\mathbf{x}, \omega)|_{\Gamma_3} &= -\frac{\partial u}{\partial \mathbf{n}}(\mathbf{x}, \omega)|_{\Gamma_4}.
 \end{aligned} \tag{2}$$

## Assumption I

The interface  $\Gamma(\omega)$  is  $C^{2,1}$ -smooth.

## Assumption II

The upper bound  $\delta_0$  is sufficiently small to ensure that the interface  $\Gamma_\delta$  is not degenerate and lies still inside the domain  $\Omega_0$ .

## Assumption III

The random field  $\kappa(\mathbf{x}, \omega)$  has a finite second moment with respect to  $P$  which belongs to the Bochner space  $L^2(\Omega, C^{2,1}(\Gamma, \mathbb{R}^2))$ .

The first order shape derivative:

$$du(\mathbf{x}) := du[\kappa](\mathbf{x}) = \lim_{\delta \rightarrow 0} \frac{u_\delta(\mathbf{x}) - u(\mathbf{x})}{\delta}, \quad \mathbf{x} \in (D^- \cap D_\delta^-) \cup (D^+ \cap D_\delta^+).$$

**Lemma 1** Under the Assumptions I–III, first order shape derivative  $du(\mathbf{x}) := d u[\kappa](\mathbf{x})$  satisfies

$$\begin{aligned}
 \bar{\mathcal{L}}du &= 0, & \text{in } D^- \cup D^+, \\
 [du] &= 0, & \text{on } \Gamma, \\
 \left[ \frac{\partial du}{\partial \mathbf{n}} \right] &= \kappa[k^2]u, & \text{on } \Gamma, \\
 du &= 0, & \text{on } \Gamma_1, \\
 du &= 0, & \text{on } \Gamma_2, \\
 du|_{\Gamma_3} &= du|_{\Gamma_4}, \\
 \frac{\partial du}{\partial \mathbf{n}}|_{\Gamma_3} &= -\frac{\partial du}{\partial \mathbf{n}}|_{\Gamma_4}.
 \end{aligned} \tag{3}$$

**Lemma 2** Under Assumptions I–III, the random solution satisfies:

$$u(\mathbf{x}, \omega) = \bar{u}(\mathbf{x}) + du[\kappa(\omega)](\mathbf{x})\delta + \frac{1}{2}d^2u[\kappa, \kappa](\mathbf{x})\delta^2 + \mathcal{O}(\delta^3), \quad (4)$$

for all  $\mathbf{x} \in K \subset \Omega_0 \setminus U_{\delta_0}(\Gamma)$ ,  $P$ -a.s.  $\omega \in \Omega$ .  $\bar{u}(\mathbf{x})$  is given by (2).

**Theorem 3** The expectation  $\mathbb{E}_u(\mathbf{x})$  of the random solutions to (3) can be approximated by

$$\mathbb{E}_u(\mathbf{x}) = \bar{u}(\mathbf{x}) + \mathcal{O}(\delta^2), \quad \mathbf{x} \in K \in \Omega_0 \setminus U_{\delta_0}(\Gamma), \quad (5)$$

Remark. Using MC-FEM or MLMC-FEM for  $\mathbb{E}_u(\mathbf{x})$  in (5).

**Theorem 4** The variance  $\text{Var}_u(\mathbf{x})$  of random solutions to (3) can be approximated by

$$\begin{aligned} \text{Var}_u(\mathbf{x}) &= \delta^2 \text{Var}_{du}(\mathbf{x}) + \mathcal{O}(\delta^3) \\ &= \delta^2 \text{Cor}_{du}(\mathbf{x}, \mathbf{y})|_{\mathbf{y}=\mathbf{x}} + \mathcal{O}(\delta^3), \quad \mathbf{x} \in \mathcal{K} \Subset \Omega_0 \setminus U_{\delta_0}(\Gamma), \end{aligned} \quad (6)$$

From (3), the deterministic tensor product PDE of  $\text{Cor}_{du}(\mathbf{x}, \mathbf{y})$  on the product domain  $\Omega_0 \times \Omega_0 \subset \mathbb{R}^{2d}$  is given by:

$$\bar{\mathcal{L}}_x \otimes \bar{\mathcal{L}}_y \text{Cor}_{du}(\mathbf{x}, \mathbf{y}) = 0,$$

for all  $(\mathbf{x}, \mathbf{y}) \in \Omega_0 \times \Omega_0$  with corresponding 20 boundary conditions.  
**Not applicable!**

## Low-rank approximation

---

**Algorithm 1:** Pivoted Cholesky decomposition

---

**Data:** matrix  $\mathbf{C} = [\text{Cor}_\kappa(\mathbf{x}_i, \mathbf{x}_j)]_{i,j} \in \mathbb{R}^{n \times n}$  and error tolerance  $\sigma > 0$   
**Result:** low-rank approximation  $\mathbf{C}_m = \sum_{i=1}^m \ell_i \ell_i^T$  such that  $\text{trace}(\mathbf{C} - \mathbf{C}_m) \leq \sigma$

```

begin
  set  $m := 1$ ;
  set  $\mathbf{d} := \text{diag}(\mathbf{C})$  and  $\text{error} := \|\mathbf{d}\|_1$ ;
  initialize  $\boldsymbol{\pi} := (1, 2, \dots, n)$ ;
  while  $\text{error} > \sigma$  do
    set  $i := \arg \max\{d_{\pi_j} : j = m, m+1, \dots, n\}$ ;
    swap  $\pi_m$  and  $\pi_i$ ;
    set  $\ell_{m, \pi_m} := \sqrt{d_{\pi_m}}$ ;
    for  $m+1 \leq i \leq n$  do
      compute  $\ell_{m, \pi_i} := \left( \text{Cor}_\kappa(\mathbf{x}_{\pi_m}, \mathbf{x}_{\pi_i}) - \sum_{j=1}^{m-1} \ell_{j, \pi_m} \ell_{j, \pi_i} \right) / \ell_{m, \pi_m}$ ;
      update  $d_{\pi_i} := d_{\pi_i} - \ell_{m, \pi_i} \ell_{m, \pi_i}$ ;
    end
    compute  $\text{error} := \sum_{i=m+1}^n d_{\pi_i}$ ;
    increase  $m := m + 1$ ;
  end
  
```

---

(I) Given the two-point correlation matrix  $\mathbf{C} = [\text{Cor}_\kappa(\mathbf{x}_i, \mathbf{x}_j)]_{i,j}$ , we obtain

$$\text{Cor}_\kappa \approx \text{Cor}_{\kappa, m} = \sum_{i=1}^m \kappa_i \otimes \kappa_i. \quad (7)$$

## Low-rank approximation: (Cont')

(II) Given  $\kappa$ , find  $du = du[\kappa] \in H_g^1(D^-) \cup H_g^1(D^+)$

$$\begin{aligned}
 & - \int_{D^+ \cup D^-} s \frac{\partial du}{\partial x_1} \frac{\partial v}{\partial x_1} d\mathbf{x} - \int_{D^+ \cup D^-} \frac{1}{s} \frac{\partial du}{\partial x_3} \frac{\partial v}{\partial x_3} d\mathbf{x} \\
 & + \int_{D^+ \cup D^-} (k^2 - |\alpha|^2) s du v d\mathbf{x} = - \int_{\Gamma} \kappa [k^2] uv d\mathbf{x}, \quad v \in H_p^1(\Omega_0).
 \end{aligned} \tag{8}$$

Linearity of the mapping  $\kappa \mapsto du[\kappa]$ .

(III) With such a low-rank approximation  $\kappa_i$  at hand, we have

$$\text{Cor}_{du} \approx \text{Cor}_{du,m} = \sum_{i=1}^m du[\kappa_i] \otimes du[\kappa_i]. \tag{9}$$

## Low-rank approximation: (Cont')

**Overall Algorithm 2:** Low rank approximation for the variance.

**Input:** matrix  $[\text{Cor}_\kappa(\mathbf{x}_i, \mathbf{x}_j)]_{i,j}$  and tolerance  $\varepsilon_0 > 0$ .

**Output:** A third order approximation of  $\text{Var}_u(\mathbf{x})$ .

(I) Compute  $\text{Cor}_\kappa \approx \sum_{i=1}^m \kappa_i \otimes \kappa_i$  by Algorithm 1.

(II) Given  $\kappa_i$ , calculate the quantity  $\text{d}u[\kappa_i]$  by weak formulation.

(III) Compute the quantity  $\text{Cor}_{\text{d}u}$  by the formula (9).

$$\text{Var}_u(\mathbf{x}) = [\text{Var}_{\text{d}u}(\mathbf{x})]\delta^2 + \mathcal{O}(\delta^3) = [\text{Cor}_{\text{d}u}(\mathbf{x}, \mathbf{y})|_{\mathbf{y}=\mathbf{x}}]\delta^2 + \mathcal{O}(\delta^3).$$

The advantage of WG method

(1) The solution itself or its gradient **changes rapidly near the interface.**

(2) The stabilizer: **the parameter is 1.**

HDGM, adjust the flux terms or penalty terms to guarantee the stability.

(3) The interfaces are always complicated.

Allows **arbitrary polygons** as the partitions are shape regular.

The convergence analysis with different polygons are guaranteed under the **same framework.**

[1] J.P. Wang and X. Ye *A weak galerkin finite element method for second-order elliptic problems*. J. Comput. Appl. Math., 241, 2013, 103-115.

**Theorem 6.** On  $K \in D \setminus U_{\sigma_0}(\Gamma)$ , there holds for the expectation  $\mathbb{E}_u$  of the random solution to the original problem (2)

$$\|\mathbb{E}_u - \bar{u}_h\| \leq C (\delta^2 + h) \|\bar{u}\|_{H^2(D_0^-) \cup H^2(D_0^+)}$$

with

$$\|v\| = \sqrt{\|\nabla_d v\|^2 + \|v_i\|^2 + s(v, v)}. \quad (10)$$

## Numerical simulation

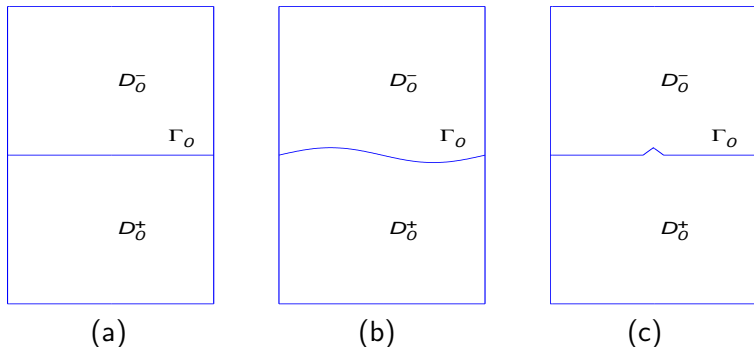


Figure: Three different kinds of nominal interfaces: (a) straight line; (b) sin-like line; (c) line with corner.

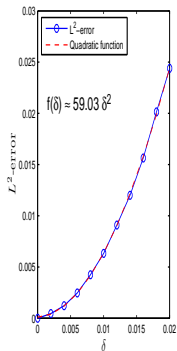
The random perturbation of the interface is assumed to exhibit the Gaussian two-point correlation

$$\text{Cor}_\kappa = \exp(-\sigma \|\mathbf{x} - \mathbf{y}\|^2)$$

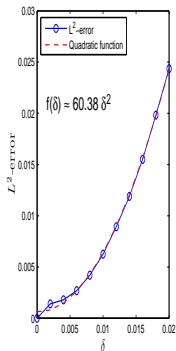
with  $\sigma = 10$ .

Here,  $k_- := 3.2\pi$  and  $k_+ := 1.6\pi$

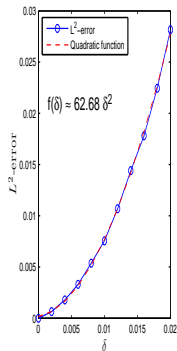
## Expectation error of three examples: $O(\delta^2)$



(a)

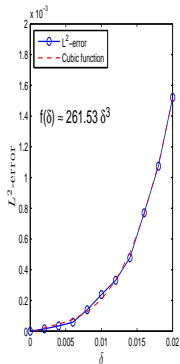


(b)

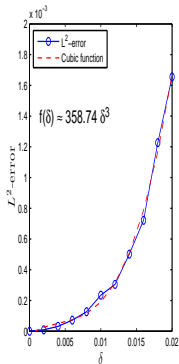


(c)

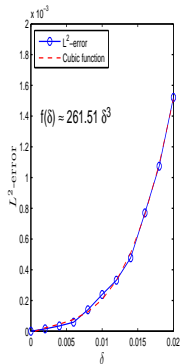
## Variance error of three examples: $O(\delta^3)$



(a)



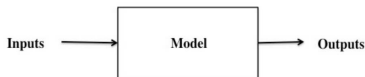
(b)



(c)

## Inverse problems

Given the **observation**, or **output**, or **expectation**.  
Determine the **cause**, or **input**, or **control**.



$\mathbb{X}$ : the set/space of quantities (functions) or shapes (geometries)—target objects.

$\mathbb{Y}$ : the set/space of data.

$F$ : a relationship/mapping from  $\mathbb{X}$  to  $\mathbb{Y}$ .

Inverse problems:

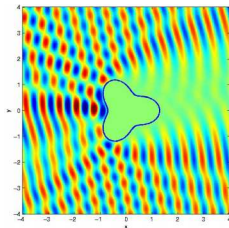
$$F(x) = y, \quad x \in \mathbb{X}, \quad y \in \mathbb{Y}.$$

Given  $y$ , find  $x$  or missing information of  $F$ .

## Inverse scattering problems

Waves, oscillations accompanied by a transfer of energy that travel through space or mass.

Fine properties: propagating, penetrating, non-destructive.



Inverse scattering problems:

$F(\text{target object}) = \text{wave field away from the object.}$

## PDE Model

Time-harmonic waves:  $\tilde{u}(x, t) = e^{i\omega t} u(x)$

$$\frac{1}{c^2} \tilde{u}_{tt} - \Delta \tilde{u} = 0 \Rightarrow \Delta u + k^2 u = 0, \quad k = \frac{\omega}{c}.$$

Acoustic scattering problems.

(a) Wave scattering from an active source:  $f = \varphi \chi_{\Omega}$ ,  $\varphi \in L^{\infty}(\mathbb{R}^n)$

$$(\Delta + k^2)u = f, \quad \lim_{r \rightarrow \infty} r^{\frac{n-1}{2}} (\partial_r - ik)u = 0, \quad r = |x|.$$

(b) Penetrable medium scattering:  $u^i(x, \theta, k) = e^{ikx \cdot \theta}$ , plane wave

$$\begin{aligned} (\Delta + k^2(1 + q))u &= 0, \quad u = u^i + u^s, \\ \lim_{r \rightarrow \infty} r^{\frac{n-1}{2}} (\partial_r - ik)u^s &= 0. \end{aligned}$$

## Acoustic scattering problems (Cont')

(c) Obstacle scattering:  $u^i(x, \theta, k) = e^{ikx \cdot \theta}$ , plane wave

$$\begin{aligned} (\Delta + k^2)u &= 0 \text{ in } \mathbb{R}^n \setminus \Omega, \quad \mathcal{B}u|_{\partial\Omega} = 0, \quad u = u^i + u^s, \\ \lim_{r \rightarrow \infty} r^{\frac{n-1}{2}} (\partial_r - ik)u^s &= 0. \end{aligned} \quad (11)$$

- ◇ Far field pattern: observation aperture  $\hat{x} := x/|x| \in \mathbb{S}^{n-1}$ ,  
 incident aperture  $\hat{\theta} \in \mathbb{S}^{n-1}$ , as  $r \rightarrow \infty$ ,

$$u^s(\Omega; x, \theta) = \frac{e^{i\frac{\pi}{4}}}{\sqrt{8k\pi}} \left( e^{-i\frac{\pi}{4}} \sqrt{\frac{k}{2\pi}} \right)^{n-2} \frac{e^{ikr}}{r^{\frac{n-1}{2}}} \left\{ u_{\infty}^s(\Omega; \hat{x}, \hat{\theta}) + \mathcal{O}\left(\frac{1}{r^{\frac{n}{2}}}\right) \right\}.$$

- ◇ inverse acoustic scattering:

(a)  $F(f) = u_{\infty}^s(\hat{x}, \hat{\theta})$ ; (b)  $F(q) = u_{\infty}^s(\hat{x}, \hat{\theta})$ ; (c)  $F(\Omega) = u_{\infty}^s(\hat{x}, \hat{\theta})$ .

## Inverse acoustic obstacle scattering problem

Incident plane wave  $u^i(x, \theta) = e^{ikx \cdot \theta}$ ,

$$(\Delta + k^2)u = 0 \text{ in } \mathbb{R}^n \setminus \Omega, \quad \mathcal{B}u|_{\partial\Omega} = 0, \quad u = u^i + u^s,$$

$$\lim_{r \rightarrow \infty} r^{\frac{n-1}{2}} (\partial_r - ik)u^s = 0.$$

- ◇ inverse acoustic obstacle scattering:

$$F(\Omega) = u_{\infty}^s(\hat{x}, \hat{\theta}), \quad (\hat{x}, \hat{\theta}) \in \Gamma \times \Sigma.$$

$\Gamma \subset \mathbb{S}^{n-1}$ : observation aperture;  $\Sigma \subset \mathbb{S}^{n-1}$ : incident aperture.

- ◇  $\Gamma = \mathbb{S}^{n-1}$  and  $\Sigma = \mathbb{S}^{n-1}$ : full-aperture data; Otherwise, **limited-aperture** data, or incomplete data.

## History: inverse scattering problems with incomplete data

Full-aperture data: [Colton and Kress, 92], uniquely determine.

Limited-aperture data: analytic function, unique continuation; severely ill-conditioned process. [Mager and Bleistein, 78,79], [Zinn, 89], [Bao and Liu, 03], etc.

- ◇ regularized homotopy continuation method: [Bao and Liu, 03]
- ◇ a variant of the enclosure method: [Ikehata, Niemi and Siltanen, 12]
- ◇ a generalization of the orthogonal projection method: [Ochs, 87]
- ◇ the methods based on transformed field expansion: [Li, Liu and Wang, 17]

## History: inverse scattering problems with incomplete data (Cont')

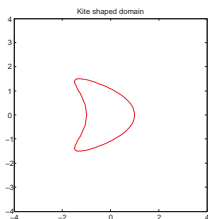
- ◇ aforesaid structures: real-analyticity and reciprocity relations
  - (1) retrieve the missing data.
  - (2) apply the existing numerical methods for the corresponding full-aperture problems. [Liu and Sun, 17]
- ◇ phaseless case: artificial reference scatterer retrieving the phase information of the measurement data. [Li, Liu and Zou, 09], [Zhang and Guo, 18], [Zhang, Guo, Li and Liu, 18], [Dong, Zhang and Guo, 19], [Ji, Liu and Zhang, 19].
- ◇ **phaseless case: ML**  
[Yin, Yang and Liu, 20], [Gao and Zhang, 21], [Yang, Gui, Ming and Hu, 20], [Gao, Liu, Wang and Zhang, 21]

## One example with incomplete data

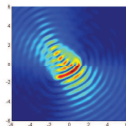
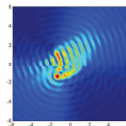
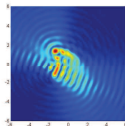
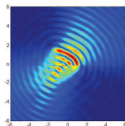
**Sampling method:** imaging functional

$$I(z) := \left| \int_{\Sigma} e^{-ik\hat{\theta}\cdot z} \int_{\Gamma} u^{\infty}(\hat{x}, \hat{\theta}) e^{ik\hat{x}\cdot z} ds(\hat{x}) ds(\hat{\theta}) \right|^2, \quad z \in \mathbb{R}^n.$$

kite:  $x(t) = (a, b) + (\cos t + 0.65 \cos 2t - 0.65, 1.5 \sin t)$ ,  $0 \leq t \leq 2\pi$ .



## One example with incomplete data (Cont')



$$\hat{x} \in (0, \pi/2), \quad \hat{x} \in (\pi/2, \pi), \quad \hat{x} \in (\pi, 3\pi/2), \quad \hat{x} \in (3\pi/2, 2\pi)$$

**Our contribution:** convolution neural network (CNN) for retrieve the missing data, even phaseless case.

## Preliminary of machine learning Developments

- ◇ Artificial neural network (ANN): [McCulloch and Pitts, 43]
- ◇ Convolutional neural networks (CNN): [LeCun et al., 88], LeNet5
- ◇ Deep neural network (DNN): [Hinton et al., 10]
- ◇ 2017, AlphaGo defeated Ke Jie.
- ◇ RNN, LSTM, etc. Powerful tools in image processing and natural language processing.

## Mathematical analysis

- ◇ “universal approximation theorem”, [Cybenko and Hornik, 89].
- ◇ Barron space, [E, Ma and Wu, 19].

## CNN notations

- ◇ Let  $\mathbf{z}_{i,j}^l$ : input patch at  $(i, j)$ ,  $l$ -th layer, picture.
- ◇  $y_{i,j,k}^l$ : feature value at  $(i, j)$ ,  $k$ -th feature map,  $l$ -th layer.

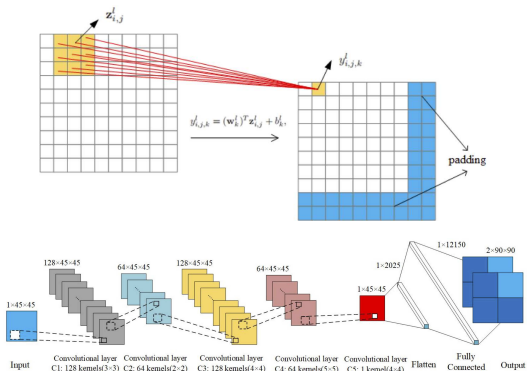
$$\begin{cases} y_{i,j,k}^l &= (\mathbf{w}_k^l)^T \mathbf{z}_{i,j}^l + b_k^l, \\ z_{i,j,k}^l &= \sigma^l(y_{i,j,k}^l). \end{cases}$$

Denote  $W = \{\mathbf{w}_k^l\}$  and  $b = \{b_k^l\}$ . The parametric rectified linear unit (PReLU)

$$\sigma(\alpha, x) = \begin{cases} \alpha \cdot x, & x < 0, \\ x, & x \geq 0, \end{cases}$$

where  $\alpha$  is a learned array with the same dimension as  $x$ .

## CNN representation



Advantage:

- (1) considering locality of features and extracting spatial features.
- (2) fixed small window size of convolutions.

## Star shaped domain

The star shaped domains

$$x(t) = r(t) \cos(t), \quad y(t) = r(t) \sin(t), \quad t \in [0, 2\pi].$$

We then represent the radius function  $r(t)$  by the truncated Fourier series expansion

$$r(t) = a_0 \left\{ 1 + \frac{1}{2N} \sum_{n=1}^N n^{-q} [a_n \cos(nt) + b_n \sin(nt)] \right\}, \quad (12)$$

where  $N \in \mathbb{N}$  is the cut-off frequency, and  $a_n, b_n, n = 1, \dots, N$  are random numbers draw from the uniform distribution in  $[-1, 1]$ .

## Multi-static response matrix

The multi-static response matrix  $\mathbb{F}_{full} \in \mathbb{C}^{2m \times 2m}$ :

$$\mathbb{F}_{full} = \begin{pmatrix} u_{1,1}^\infty & u_{1,2}^\infty & \cdots & u_{1,2m}^\infty \\ u_{2,1}^\infty & u_{2,2}^\infty & \cdots & u_{2,2m}^\infty \\ \vdots & \vdots & \ddots & \vdots \\ u_{2m,1}^\infty & u_{2m,2}^\infty & \cdots & u_{2m,2m}^\infty \end{pmatrix},$$

where  $u_{i,j}^\infty = u_\infty^s(\hat{x}_j; \hat{\theta}^i)$  for  $1 \leq i, j \leq 2m$  corresponding to  $2m$  observation directions  $\hat{x}_j$  and  $2m$  incident directions  $\hat{\theta}^i$ .

Generally speaking, we can partition into a 2-by-2 block matrix

$$\mathbb{F}_{full} = \begin{pmatrix} \mathbb{F}_{11} & \mathbb{F}_{12} \\ \mathbb{F}_{21} & \mathbb{F}_{22} \end{pmatrix}, \quad (13)$$

where  $\mathbb{F}_{11} \in \mathbb{C}^{m_1 \times m_1}$ ,  $\mathbb{F}_{12} \in \mathbb{C}^{m_1 \times m_2}$ ,  $\mathbb{F}_{21} \in \mathbb{C}^{m_2 \times m_1}$ ,  $\mathbb{F}_{22} \in \mathbb{C}^{m_2 \times m_2}$ , and  $m_1 + m_2 = 2m$ .

## Algorithm development

- (I) Using (12), generate the random domain.
- (II) Using FEM to solve obstacle scattering (11), and then obtain  $\mathbb{F}_{full}$ .
- (III) **Using CNN** retrieve the missing data.
- (IV) Apply the existing numerical methods for the corresponding full-aperture problems.

## Notations 1: $\mathcal{L}_1$

- ◇ sample set:  $n^*$ ; train set:  $n_1$ ; test set:  $n_2$ .
- ◇ Given the input data  $x = \mathbb{F}_{12}^n \in \mathbb{R}^{m_1 \times m_1 \times 2}$  and the target outputs  $y = [\mathbb{F}_{11}^n, \mathbb{F}_{12}^n; \mathbb{F}_{21}^n, \mathbb{F}_{22}^n] \in \mathbb{R}^{2m \times 2m \times 2}$  in the training set, we wish  $y^C(x; W, b) \approx y(x)$ , where  $y^C(x; W, b) = [\mathbb{F}_{11}^{n,C}, \mathbb{F}_{12}^{n,C}; \mathbb{F}_{21}^{n,C}, \mathbb{F}_{22}^{n,C}]$ .

◇

$$\mathcal{L}_1(y, y^C) = \frac{1}{n_1} \sum_{n=1}^{n_1} \sum_{i,j=1}^2 \|\mathbb{F}_{ij}^n - \mathbb{F}_{ij}^{n,C}\|_F^2, \quad (14)$$

where  $\|\cdot\|_F$  is the Frobenius norm of a matrix.

- ◇ We use the CNN to compute

$$W^*, b^* = \arg \min_{W, b} \mathcal{L}_1(y, y^C),$$

with the Adam optimizer.

## Notations 2: sub-block relative errors

We define the following sub-block relative errors

$$e_{11}^n = \frac{\|\mathbb{F}_{11}^n - \mathbb{F}_{11}^{n,C}\|_F}{\|\mathbb{F}_{11}^n\|_F}, \quad e_{21}^n = \frac{\|\mathbb{F}_{21}^n - \mathbb{F}_{21}^{n,C}\|_F}{\|\mathbb{F}_{21}^n\|_F}, \quad e_{22}^n = \frac{\|\mathbb{F}_{22}^n - \mathbb{F}_{22}^{n,C}\|_F}{\|\mathbb{F}_{22}^n\|_F},$$

$$n = n_1 + 1, \dots, n^*$$

for each sample in the test set, and use the sub-block relative errors of the test set

$$\bar{e}_{11} = \frac{1}{n_2} \sum_{n=n_1+1}^{n^*} e_{11}^n, \quad \bar{e}_{21} = \frac{1}{n_2} \sum_{n=n_1+1}^{n^*} e_{21}^n, \quad \bar{e}_{22} = \frac{1}{n_2} \sum_{n=n_1+1}^{n^*} e_{22}^n,$$

to check the efficiency of our CNN.

## Notations 3: $e^n$ , $MSE^n$ , and $PSNR^n$

- ◇ The recovery multi-static response matrix is

$$\tilde{\mathbb{F}}_{full}^n = \begin{pmatrix} \mathbb{F}_{11}^{n,C} & \mathbb{F}_{12}^n \\ \mathbb{F}_{21}^{n,C} & \mathbb{F}_{22}^{n,C} \end{pmatrix}, \quad n = n_1 + 1, \dots, n^*,$$

for each sample in the test set.

- ◇ Given  $\mathbb{F}_{full}^n$  and  $\tilde{\mathbb{F}}_{full}^n$ , define

$$e^n = \frac{\|\mathbb{F}_{11}^n - \mathbb{F}_{11}^{n,C}\|_F + \|\mathbb{F}_{21}^n - \mathbb{F}_{21}^{n,C}\|_F + \|\mathbb{F}_{22}^n - \mathbb{F}_{22}^{n,C}\|_F}{\|\mathbb{F}_{11}^n\|_F + \|\mathbb{F}_{21}^n\|_F + \|\mathbb{F}_{22}^n\|_F},$$

$$MSE^n = \frac{1}{2m \cdot 2m} \sum_{i=1}^{2m} \sum_{j=1}^{2m} \left| \mathbb{F}_{full}^n(i, j) - \tilde{\mathbb{F}}_{full}^n(i, j) \right|^2,$$

$$PSNR^n = 10 \cdot \log_{10} \left( \frac{\max_{i,j} |\mathbb{F}_{full}^n(i, j)|}{MSE^n} \right).$$

## Notations 4: $\bar{e}$ , $\overline{\text{MSE}}$ , and $\overline{\text{PSNR}}$

Introduce the relative error, mean square error (MSE), and peak signal-to-noise ratio (PSNR) of the test set as follows:

$$\bar{e} = \frac{1}{n_2} \sum_{n=n_1+1}^{n^*} e^n,$$

$$\overline{\text{MSE}} = \frac{1}{n_2} \sum_{n=n_1+1}^{n^*} \text{MSE}^n,$$

$$\overline{\text{PSNR}} = \frac{1}{n_2} \sum_{n=n_1+1}^{n^*} \text{PSNR}^n.$$

## Two numerical simulations

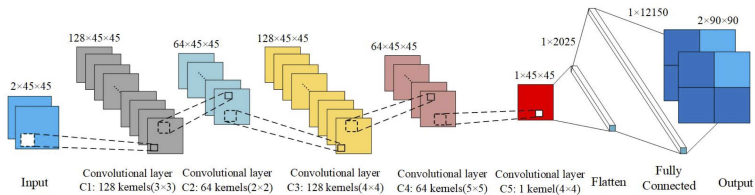
(I) Standard optimization functional.

(II) Phaseless case.

We take  $N = 5$ ,  $q = 0$ , and  $a_0$  to be a random number drawn from the uniform distribution in  $[0.5, 1.5]$  under (12).

## Example 1: Standard optimization functional

$$n^* = 20000, m_1 = m_2 = 45, \mathcal{L}_1 = \mathcal{L}_1(y, y^C).$$



## Example 1: sub-block relative errors

Table: 1. The sub-block relative errors of test set in Example 1.

$(n_1, n_2)$	error real(%)			error image(%)		
	$\bar{e}_{11}$	$\bar{e}_{21}$	$\bar{e}_{22}$	$\bar{e}_{11}$	$\bar{e}_{21}$	$\bar{e}_{22}$
(2000,500)	26.01	84.15	26.01	30.72	86.03	30.71
(4000,1000)	19.01	67.55	19.00	22.49	68.43	22.49
(8000,2000)	14.22	51.15	14.22	16.88	52.12	16.88
(16000,4000)	10.66	38.88	10.66	12.61	39.82	12.61

$(n_1, n_2)$	error norm(%)		
	$\bar{e}_{11}$	$\bar{e}_{21}$	$\bar{e}_{22}$
(2000,500)	28.06	84.99	30.71
(4000,1000)	20.52	67.92	20.52
(8000,2000)	15.38	51.54	15.38
(16000,4000)	11.50	39.27	11.50

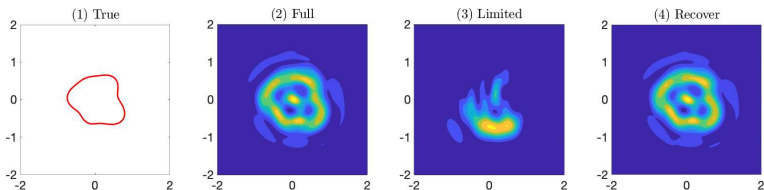
## Example 1: $\bar{e}$ , $\overline{\text{MSE}}$ , and $\overline{\text{PSNR}}$

Table: 2. The relative errors,  $\overline{\text{MSE}}$ s, and  $\overline{\text{PSNR}}$ s of test set in Example 1.

$(n_1, n_2)$	relative error $\bar{e}$ (%)			$\overline{\text{MSE}}(10^{-2})$		
	real	image	norm	real	image	norm
(2000,500)	39.13	44.03	41.40	9.372	9.384	5.430
(4000,1000)	34.06	38.47	36.11	6.979	7.042	4.371
(8000,2000)	23.97	27.09	25.41	3.445	3.440	2.594
(16000,4000)	16.63	18.80	17.63	1.691	1.692	1.365

$(n_1, n_2)$	$\overline{\text{PSNR}}$		
	real	image	norm
(2000,500)	19.21	16.22	22.37
(4000,1000)	20.28	17.27	22.24
(8000,2000)	23.24	20.22	25.65
(16000,4000)	26.46	23.46	28.63

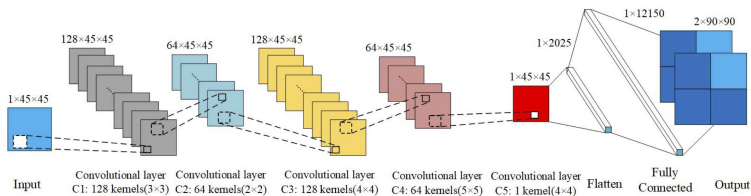
## Example 1: pictures



**Figure:** Numerical constructions of the 1st shape in the test set. (1) the true shape; (2) reconstructed shape from the full MSR matrix  $\mathbb{F}_{full}^n$ ; (3) reconstructed shape from the limited MSR matrix  $\mathbb{F}_{12}^n$ ; (4) reconstructed shape from the recovered MSR matrix  $\widetilde{\mathbb{F}}_{full}^n$  via CNN.

## Example 2: Phaseless case

$n^* = 50000$ ,  $m_1 = m_2 = 45$ , Optimization functional  $\mathcal{L}_2$  is same as Example 1. The input is the module.



## Example 2: the relative errors $\bar{e}$ and $\overline{\text{MSE}}$

Table: 3. Phase and phaseless in Example 2 with regularization term.

$(n_1, n_2)$	relative error $\bar{e}$ (%)			$\overline{\text{MSE}}(10^{-2})$		
	real	image	norm	real	image	norm
(5000,1250)	30.08	33.63	33.73	5.372	5.319	3.686
(10000,2500)	21.71	24.43	22.97	2.869	2.852	2.128
(20000,5000)	15.26	17.17	16.14	1.390	1.383	1.149
(40000,10000)	12.00	13.45	12.67	0.798	0.786	0.677

$(n_1, n_2)$	relative error $\bar{e}$ (%)			$\overline{\text{MSE}}(10^{-2})$		
	real	image	norm	real	image	norm
(5000,1250)	57.49	64.95	60.91	20.535	20.615	11.332
(10000,2500)	46.92	53.41	49.90	12.562	12.719	6.648
(20000,5000)	41.77	47.73	44.51	9.860	10.008	5.266
(40000,10000)	37.97	43.28	40.40	7.510	7.573	4.408

## Example 2: $\overline{\text{PSNR}}$

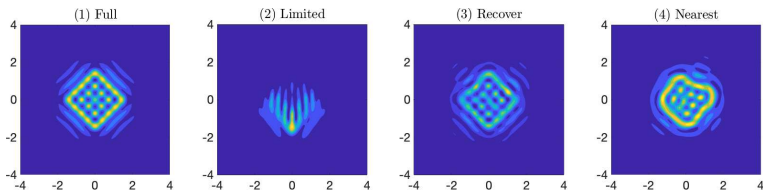
Table: 4. Phase and phaseless in Example 2 with regularization term.

	$\overline{\text{PSNR}}$		
$(n_1, n_2)$	real	image	norm
(5000,1250)	21.34	18.47	23.91
(10000,2500)	24.16	21.18	26.64
(20000,5000)	27.12	24.18	29.30
(40000,10000)	29.02	26.10	31.20

	$\overline{\text{PSNR}}$		
$(n_1, n_2)$	real	image	norm
(5000,1250)	15.87	12.84	20.24
(10000,2500)	17.33	14.23	21.65
(20000,5000)	18.30	15.18	22.55
(40000,10000)	18.91	15.81	22.91

## Example 2: pictures



**Figure:** Numerical constructions for square-shape obstacle by (1) the full MSR matrix  $\mathbb{F}_{full}^c$ ; (2) the limited MSR matrix  $\mathbb{F}_{12}^c$ ; (3) the recovery MSR matrix  $\widetilde{\mathbb{F}}_{full}^c$  via CNN; (4) nearest sample MSR matrix  $\widetilde{\mathbb{F}}_{full}^{c*}$ .

matrix type	relative error (%)		
	real	image	norm
$\widetilde{\mathbb{F}}_{full}^s$	32.00	30.42	31.25
$\widetilde{\mathbb{F}}_{full}^{s*}$	66.75	69.21	67.94

## Reference

- ▶ G. BAO, Y.Z. CAO, Y.L. HAO, AND K. ZHANG, [A robust numerical method for the random interface grating problem via shape calculus, weak Galerkin method, and low-rank approximation](#). *J Sci. Comput.*, **77(1)**, 2018, 419-442.
- ▶ Y.L. HAO, F.D. KANG, J.Z. LI AND K. ZHANG, [Computation of moments for Maxwell's equations with random interfaces via pivoted low-rank approximation](#). *J Comput. Phys.*, **371**, 2018, 1-18.
- ▶ Y. GAO AND K. ZHANG, [Machine learning based data retrieval for inverse scattering problems with incomplete data](#). *J Inverse Ill Posed Probl*, **29(2)**, 2021, 249-266.
- ▶ Y. GAO, H.Y. LIU, X.C. WANG AND K. ZHANG, [On an artificial neural network for inverse scattering problems](#). *J Comput. Phys.*, **448**, 2022, 110771.

## Conclusions

- ▶ Random interface grating.
  - ▶ Expectation approximation: Taylor shape expansion,  $O(\delta^2)$ .
  - ▶ Variance approximation: Low-rank Cholesky method,  $O(\delta^3)$ .
- ▶ ML for inverse acoustic scattering problem.
  - ▶ Obstacle: CNN.

## Ongoing works

Bayesian inverse problem for defect and crack in waveguided.

# Thank you!

zhangkaimath@jlu.edu.cn